Research Article

Metastable atom-activated dissociation mass spectrometry: leucine/isoleucine differentiation and ring cleavage of proline residues

Shannon L. Cook, Olivier L. Collin and Glen P. Jackson*

Extensive backbone fragmentation resulting in a-, b-, c-, x-, y- and z-type ions is observed of singly and doubly charged peptide ions through their interaction with a high kinetic energy beam of argon or helium metastable atoms in a modified quadrupole ion trap mass spectrometer. The ability to determine phosphorylation-sites confirms the observation with previous reports and we report the new ability to distinguish between leucine and isoleucine residues and the ability to cleave two covalent bonds of the proline ring resulting in a-, b-, x-, y-, z- and w-type ions. The fragmentation spectra indicate that fragmentation occurs through nonergodic radical ion chemistry akin to electron capture dissociation (ECD), electron transfer dissociation (ETD) and electron ionization dissociation mechanisms. However, metastable atom-activated dissociation mass spectrometry demonstrates three apparent benefits to ECD and ETD: (1) the ability to fragment singly charged precursor ions, (2) the ability to fragment negatively charged ions and (3) the ability to cleave the proline ring that requires the cleavage of two covalent bonds. Helium metastable atoms generated more fragment ions than argon metastable atoms for both substance P and bradykinin regardless of the precursor ion charge state. Reaction times less than 250 ms and efficiencies approaching 5% are compatible with on-line fragmentation, as would be desirable for bottom-up proteomics applications. Copyright © 2009 John Wiley & Sons, Ltd.

Supporting information may be found in the online version of this article.

Introduction

Recent advances in mass spectrometry have provided unprecedented investigative power for biomedical and clinical researchers. In tandem mass spectrometry, a mass-to-charge relationship is established between the product ions of a reaction and the precursor ions from which they originated, and there are three fundamental processes by which precursor gas-phase ions can be made to fragment: (1) collisions with atoms, molecules or surfaces[1,2]; (2) photodissociation[3–6]; and (3) dissociative-recombination with an oppositely charged species.[7,8] Table 1, adapted from Ref. [9], summarizes these methods, including the fragmentation method promulgated in this work: metastable atom-activated dissociation (MAD).

Of these activation methods, collision-induced dissociation (CID), also called collision-activated dissociation (CAD), is the most widely used method.[1,9] CID of peptides and small proteins has been extensively studied and the major fragmentation pathways are well known.[10–13] CID in radiofrequency (rf)-trapping instruments is classified as a 'slow-heating' excitation method.[14] The fragmentation process in these instruments is a result of multiple collisions of the ions with neutral gas atoms and peptide cleavage occurs mostly at the weakest bonds, forming mainly b-/y-type ions. The charge state of proteins undergoing CID also plays a significant yet unpredictable role in determining the fragmentation pathways.[15–17] Although whole proteins can often be identified using CID, complete sequence coverage is rarely obtained. Posttranslational modifications such as phosphorylation are often not pinpointed in CID because they are often lost during fragmentation.[18]

The capture of low kinetic energy electrons by multiply charged peptide cations has been demonstrated to result in effective cleavage of the peptide backbone.[8] This approach, called electron capture dissociation (ECD), is the new preferred method of sequencing peptides in expensive Fourier transform ion cyclotron resonance (FT-ICR) instruments[8,19] and, more recently, in an off-axis linear ion trap by Hitachi.[20] One advantage of ECD is the extensive fragmentation along the amide backbone[21] resulting in mainly c-/z-type ions that has been shown to generate more complete amino acid sequence coverage of peptides than conventional collisional activation. A drawback of ECD is that it sometimes favors certain fragmentation pathways such as on the C-terminal side of tryptophan.[22,23] Hot ECD (HECD) has the ability to impart more kinetic energy into peptide fragmentation leading to more fragmentation than is achieved in conventional ECD and can sometimes differentiate between isoleucine and leucine.[24,25]

* Correspondence to: Glen P. Jackson, Center for Intelligent Chemical Instrumentation, Department of Chemistry and Biochemistry, Ohio University, Athens, OH 45701-2979, USA. E-mail: jacksong@ohio.edu

Center for Intelligent Chemical Instrumentation, Department of Chemistry and Biochemistry, Ohio University, Athens, OH 45701-2979, USA

1211

Table 1. Comparison of demonstrated activation techniques for peptide and protein precursor ions

Activation method	Energy range	Ion charge	Instruments	Comments
PSD	Low	+/−	ReTOF	Metastable decay caused by excess internal energy from ionization.
CID (CAD)	Low	+/−	IT, FT-ICR, QqX	Controlled-energy (1–100 eV$_{lab}$) collisions with inert gases.
	High		TOF/TOF, sectors	Same, but keV energies.
SID	Low	+/−	XqQ, IT, FT-ICR	1–100 eV$_{lab}$ collisions between ions and a metal or SAM surface.
	High		TOF/TOF, sectors	Same, but at keV energies.
IRMPD	Low	+/−	IT, FT-ICR	IR laser slowly raises internal energy of ions above dissociation thresholds.
BIRD	Low	+/−	IT, FT-ICR	Heated systems used as IR source to achieve similar consequences as IRMPD.
UV-laser	High	+/−	IT, FT-ICR	Absorption of UV photon leads to significant fragmentation of peptide backbone.
ETD	Low or High	>2+	IT, FT-ICR	Positively charged precursor ions capture an electron from reagent anions; radical ion chemistry follows.
ECD	Low	>2+	FT-ICR, QqX, IT	Capture of low-energy electrons by positive ions; radical ion chemistry follows.
EDD	High	+	QIT, FT-ICR	Electron-ion fragmentation of anions or cations.
EID		−		
MAD/MIDI	Low or High	>2+, +, <2−	IT	Metastable atoms used to add electrons to polycations or to remove electrons from singly charged cations or polyanions. Radical ion chemistry follows electron ejection/transfer.

PSD, post-source decay; CID, collision-induced dissociation; CAD, collision-activated dissociation; SID, surface-induced dissociation; ECD, electron capture dissociation; IRMPD, infrared multiphoton dissociation; BIRD, blackbody infrared radiative dissociation; ETD, electron transfer dissociation; EDD, electron-detachment dissociation; EID, electron ionization dissociation; MAD, metastable atom-activated dissociation; MIDI, metastable induced dissociation of ions; ReTOF, reflectron time-of-flight; IT, linear or quadrupole ion trap; FT-ICR, fourier transform ion cyclotron resonance; QqX, mass selective quadrupole followed by rf-only multipole followed by any mass analyzer; TOF/TOF, tandem time-of-flight; XqQ, any mass selective device followed by an rf-only multipole followed by a mass selective quadrupole; SAM, self-assembled monolayer.

The major down sides to ECD are that it has only been developed on rather expensive instrument platforms, and that ECD is not applicable to singly charged or negatively charged precursor ions. Recently, ECD, including HECD and electron-detachment dissociation (EDD) have been developed in the linear ion trap time-of-flight mass spectrometer, but the techniques are still in development.[26,27]

To overcome the limitation of trapping low-mass electrons in rf-operated ion traps, it has been demonstrated that certain radical anions can serve as effective vehicles for electron transfer reactions that result in fragmentation of the polycationic precursor ions.[28,29] Electron transfer dissociation (ETD) has been proven to work very effectively for small to medium size polycationic peptides.[30,31] Larger bio-ions tend to undergo simple charge-reduction reactions instead of fragmentation when reacted with xenon cations or small organic anions.[32,33] In 2005, the orbitrap mass analyzer was made commercially available by Thermo, rivaling the high resolution and high mass-accuracy of the FT-ICR instruments.[34] The orbitrap has recently been adapted with a linear ion trap to achieve ETD, which results in c-/z-type fragmentation and preserves posttranslational modifications.[35]

The ability to sequence anions as well as cations can be an important advantage when analyzing highly acidic or modified peptides. EDD achieves peptide fragmentation through electronic excitation of anions from electron–anion collisions, leading to radical formation and inter-residue N–C$_\alpha$ and C$_\alpha$–C bond cleavage.[36] Although a-/x-type ions are predominately detected, there are some fragments that have yet to be detected, such as d-type ions.[37] Electron excitation dissociation (EED)[24] and electron ionization dissociation (EID)[38] use a high kinetic energy beam of electrons to excite or ionize precursor peptide ions and induce fragmentation. EED fragmentation is similar to UV photodissociation and yields mainly a-type ions, whereas EID achieves side chain and backbone fragmentation, mainly in the form of c-/z-type ions and a-/x-type ions.[38]

Leucine and isoleucine differentiation has been thoroughly examined during the past few decades, by high- and low-energy CID,[39,40] fast atom bombardment (FAB),[41] HECD[25] and through the formation of metal complexes.[42,43] FAB and low-energy CID, which can be implemented on linear and quadruple trap instruments, require MS^n of the low-mass, labile immonium ion (86 m/z) of Xle (Leu or Ile) residues to differentiate the two amino acids.[39,40] To date, only small peptides containing one Xle residue or those peptides with Xle as the N-terminal residue have been readily characterized. High-energy CID and HECD are able to produce high-energy fragments, such as d- and w-type ions, which can differentiate the Xle residue.[25] However, commercial access to these dissociation methods requires expensive sector or FT-ICR instruments, respectively.

It is widely known that both ECD and ETD induce secondary fragmentation leading to side chain fragments and Xle differentiation, yet cleavage within the proline amino acid residue is rarely seen.[44] Proline is the only naturally occurring amino acid that forms a five-membered ring with its three carbon alkyl chain and the peptide backbone. Peptide backbone cleavage of the proline residue to produce a-/x- and b-/y-type ions occurs through a single covalent bond cleavage and y-ions are indeed readily observed with low-energy dissociation methods such as CID and infrared multiphoton dissociation (IRMPD) photodissociation.[45,46] However, for the formation of c-/z-type ions, two covalent bonds must be broken, one among the peptide backbone and the other within the proline ring structure itself. To our knowledge, this type of side chain cleavage resulting in z- and w-type ions has been observed only once by Cooper *et al.* using ECD and HECD.[44] MAD now

offers an alternative method for the generation of not only d- and w-type ions from the Xle residue, but z- and w-type ions from proline residues.

In 2005/2006, several groups proposed the use of metastable atoms as a method for imparting energy to precursor ions to induce fragmentation.[47–49] Misharin *et al.* noted that the exposure of precursor peptide ions to the beam of a FAB source within a quadrupole ion trap lead to effective c-/z-type fragments of peptide cations and a-/x-type fragments of peptide anions.[49] For peptide cations, the mechanism proposed is electron transfer from fast moving metastable atoms to the polypeptide cations, resulting in ETD-like fragmentation. For peptide anions, the proposed mechanism is electron detachment caused by collisions with metastable atoms (e.g. Penning ionization). In both cases, the generation of a radical on the peptide backbone led to the observed fragmentation spectra. Berkout[47] obtained similar results on a linear ion trap coupled to a time-of-flight mass spectrometer using a low kinetic beam of metastable atoms in the range of 0.05–0.1 eV. They showed that the number of c-/z-type products was superior to ETD reactions on FT-ICR instruments, especially for peptides in the 2+ charge state. More recently, Berkout and Doroshenko[48] confirmed our proposed mechanisms[50] for the Penning ionization of singly protonated precursor peptide ions and subsequent fragmentation. This most recent work demonstrates a unique capability for metastable atom activation over ECD and ETD; the ability to fragment singly charged precursor ions. In contrast to work by Berkout *et al.*, our work is performed in a modified quadrupole ion trap mass spectrometer

and with a high kinetic energy beam of metastable atoms in the range of 6–10 keV. The results agree with former observations and hypotheses and demonstrate that the efficiencies and data acquisition rates are quite compatible with those required for on-line use with liquid-phase separations such as HPLC. We note a new observation for MAD-MS; the ability to distinguish between isoleucine and leucine and to generate w- and z-ions from proline residues.

Experimental

Instrumentation

All experiments were performed on a modified Bruker EsquireLC QIT MS (Bruker Daltonics, Bremen, Germany) as shown in Fig. 1(a). The trap was modified in a similar manner to that reported elsewhere.[49,50] A 2-mm hole was drilled in the ring electrode to permit metastable atoms to enter the trap. The rf-matching network did not require retuning after this modification, but the mass axis did require recalibration using a standard tune mix solution (Agilent, Santa Clara, CA). An Ion Tech (P50 PSU, Teddington, UK) FAB gun was used as the metastable atom source. The FAB gun was removed from its original housing, leaving the existing 1 MΩ resistor attached to the anode. A collar spacer was fabricated in house to attach the FAB gun to the vacuum chamber lid of the mass spectrometer. The exit orifice of the FAB gun was approximately 2 cm above the ring electrode. Two flat-ended 4–40 screws, used as deflection electrodes, were
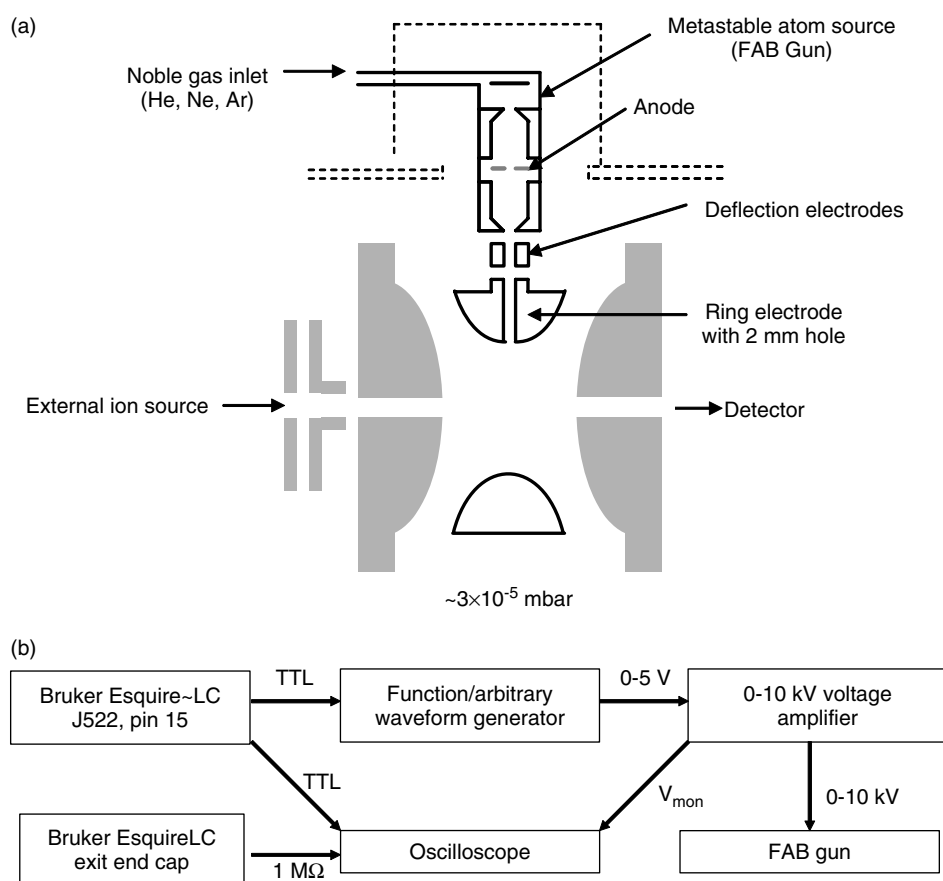

Figure 1. Schematic representation of (a) the instrument used in this study and (b) electronic components used to power the fast atom bombardment gun for pulsed operation.

mounted in tapped holes in a polyetheretherketone (PEEK) sleeve, which was mounted with a set screw on the bottom of the FAB gun. The electrodes were positioned ∼1 cm downstream of the exit orifice of the FAB gun, orthogonal to the FAB beam, with an interelectrode spacing of ∼5 mm. One electrode was grounded and the other was biased to ∼800 V using a high-voltage power supply (EL 03R 15L, Glassman High Voltage Inc., High Bridge, NJ).

Before use each day, the FAB gun was turned on for 20–30 min to 'burn' away residual contaminants such as pump oil. This helped decrease background ion signals. The Ion Tech power supply was modified slightly to permit operation at 110 V instead of the default 240 V. The presence of an active beam was measured at all times using the Ion Tech power supply through the E_{mon} connector. For pulsed operation, the anode power supply was replaced with a 10 kV high-voltage amplifier (ANT 10B10, Matsusada Precision Inc., Shiga, Japan), as shown in Fig. 1(b). The rise and fall time of this amplifier are specified as >360 V/ms, yet oscilloscope readings demonstrated considerably faster rates than this; the rise and fall times were greater than 7 kV/ms. A trigger was taken from pin 15 of connector J522 of the Bruker EsquireLC and fed to a function/arbitrary waveform generator (33 250A, Agilent, Santa Clara, CA) through 1 MΩ termination. The function generator was used to generate either a single 50–300 ms pulse or a burst of multiple 5 ms (50% duty cycle) pulses to the high-voltage power amplifier. The delay time and pulse width of the FAB gun were continually compared with the timing of the scan functions of the ion trap exit end-cap. The FAB gun was timed to be on during the section of the scan function that is normally reserved for collisional activation. To accomplish metastable atom activation at any chosen low-mass cut-off (LMCO) value, the fragmentation amplitude was set to zero volts after ion isolation and the 'fragmentation' or exposure time could be made as long as desirable (550 ms was the longest studied) at the desired LMCO value.

The FAB gun and auxiliary deflection electrodes were also characterized off-line by positioning the exit orifice of the FAB gun 3 cm above an electron multiplier (5900 Magnum, Burle, Sturbridge, MA) in a custom-modified vacuum chamber (Teledyne, Thousand Oaks, CA). Preliminary results showed that approximately 10–20% of the ion signal on the electron multiplier could be removed with a deflection voltage of 400 V/cm, with no additional reduction in ion signal at higher deflection voltages (up to 3000 V/cm). This observation is consistent with theoretical calculations for the deflection of argon ions from the beam, which show this electric field strength to be more than capable of deflecting 8 keV argon ions to a nontransmitting angle. This study suggests that argon ions make up a small proportion of the species capable of producing secondary electrons at the surface of the electron multiplier. We assume that the remaining 80–90% of the active species detected in this off-line study are either metastable or Rydberg states, as proposed by Misharin and coworkers.[49] The FAB gun and deflection plates were also characterized on-line with the ion trap with the electrospray ionization source (ESI) not in use. With a LMCO set at 18 m/z, many low-mass ions could be generated from the neutral beam with a pulse as short as 2 ms. The ions observed in this experiment are formed as a result of Penning ionization of residual gases and pump oil within the trap. Low-mass negative ions were also observed in negative ion mode with the FAB gun on. These ions could also be actively removed from the trap by employing a LMCO value above 150 m/z. The background signal was larger when using helium as the excitation source rather than argon, consistent with the fact that helium metastable

atoms have greater potential energy and can Penning ionize more substances. By raising the LMCO to 250 m/z, the background noise could be reduced to consistently low/negligible levels. The subsequent reduced intensity of the background peaks enabled the observation of product ions above the set LMCO. Turning the FAB gun on for prolonged periods before use significantly reduced the background signals.

Reagents

Bradykinin, substance P and fibrinopeptide were purchased from Sigma-Aldrich (St Louis, MO). The phosphorylated and nonphosphorylated standards of angiotensin II and cholecystokinin (10–20) were provided by Protea Biosciences Inc. (Morgantown, WV). The synthetic peptides, PHPRI and PHPRL, were donated from Dr Ralf Hoffmann (University of Leipzig, Germany). Methanol (HPLC grade) and glacial acetic acid were also purchased from Sigma-Aldrich (St Louis, MO). All peptides were reconstituted in a 1 : 1 mixture of methanol and water with 1% acetic acid to provide solutions between 10 and 25 μM of the individual peptides. Ultra high-purity helium and argon (Airgas, Parkersburg, WV) were further purified during use with a noble gas purifier (HP2, VICI, Houston, TX).

Method

The singly and doubly protonated species of each peptide were generated through ESI at a flow rate of 0.4 ml/min, provided with an electronic syringe pump (BM-1000, Protea Bioscience Inc, Morgantown, WV). A mass isolation window of 1 m/z was used to isolate the precursor ions before exposing them to the metastable atom beam at an LMCO value of 200–250 m/z. A pulsed metastable beam was applied for 200–550 ms, depending on the charge state of the precursor ion and the type of metastable atoms used. The pressure in the vacuum chamber, outside the ion trap, was kept at ∼1.3 mbar with helium as the bath gas (leaking out of the trap) and an additional 2 mbar (uncorrected) of the noble gas from the metastable atom source. The anode in the FAB gun was powered at 7 keV, unless otherwise stated, giving an instantaneous feedback current reading on the monitor electrode of ∼0.2 mA. Fragmentation data were typically acquired in 1–5 min intervals. In addition to the MAD-MS spectra of each peptide, background spectra and negative controls were also obtained for each peptide. These included (1) positive ion mode with FAB gun on and ESI source off, (2) negative ion mode with FAB gun on and ESI source off, and (3) positive ion mode with FAB source off and ESI and isolation on, to ensure fragmentation does not occur in the absence of metastable atoms and to provide a reference precursor ion signal from which MAD-MS efficiencies could be calculated. All fragment identifications and assignments were manually determined based on predicted fragmentation patterns and were within ±0.8 m/z of the expected product ions. Peaks were only assigned if the intensities were at least three times the signal-to-noise ratio. Doubly charged ions were identified according to the expected m/z value and the presence of an isotope envelope peak at +0.5 m/z.

Results and Discussion

Bradykinin: 1+ and 2+ charge states

Figure 2 shows four different MAD-MS fragmentation spectra of bradykinin. Each charge state, whether dissociated with helium
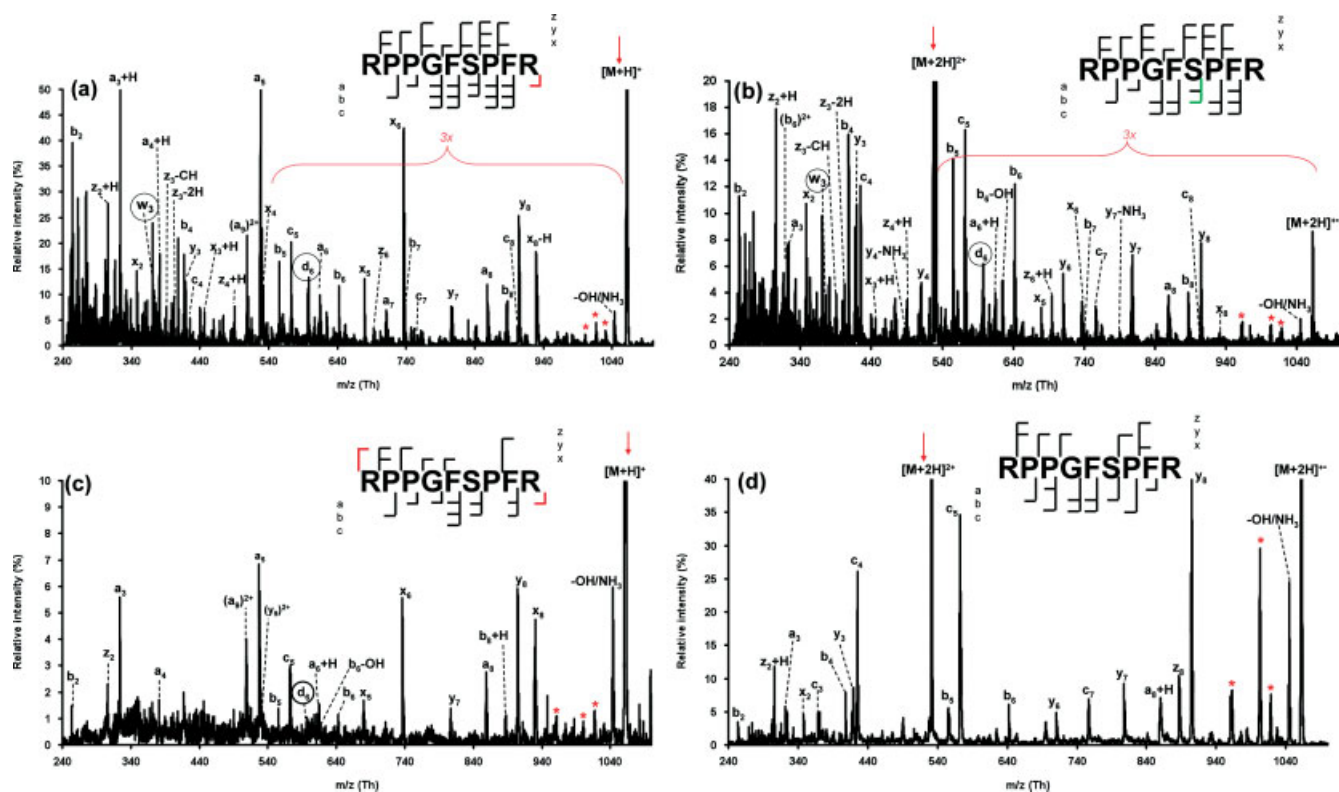
Figure 2. Metastable atom-activated dissociation spectra of bradykinin: (a) He^m+ $[M+H]^+$; (b) He^m+ $[M+2H]^{2+}$; (c) Ar^m+ $[M+H]^+$; and (d) Ar^m+ $[M+2H]^{2+}$. (Key for peptide sequencing: black line, product ions observed in $1+$ charge state; red line, product ions observed in $2+$ charge state; green line, product ions observed in both $1+$ and $2+$ charge states; precursor is indicated by a red arrow; and side chain fragments are circled).

or argon metastable atoms achieved at least 100% sequence coverage [One cleavage between every amino acid residue is defined as 100% coverage. Since, in theory, it is possible to cleave each residue in six different ways (a, b, c, x, y and z), it is possible to achieve 100% sequence coverage in $6^{n-1}-2^m$ different permutations, where n is the number of amino acids and m is the number of proline residues not on the N-terminus (proline cannot ordinarily give c- or z-type ions). Because it is also possible to obtain complete sequence coverage of a peptide using independent permutations of cleavages (i.e. all a-type cleavages or all z-type cleavages), it is hypothetically possible to achieve 100% sequence coverage up to six times over.]. MAD fragmentation efficiencies were calculated based on the relative intensities of the product ions and isolated precursor ion relative to the precursor ion signal, as described by Yost and Fetterolf[51] For bradykinin, the efficiencies ranged from 0.9 to 1.3%. Combining the fragmentation products for the $1+$ and $2+$ charge states gave a total of 33 a-, b-, c-, x-, y- and z-type fragments out of a possible 48 fragments with three different side chain fragments. MAD of the $2+$ charge state using a helium metastable beam resulted in a variety of ions (a, b, c, x, y and z) and a relatively low abundance of the charge-reduced species, $[M+2H]^{+\bullet}$. MAD of the $1+$ charge state of bradykinin yielded a higher number of fragment ions, mainly increasing the number of a-type ions detected. C_α—C and N–C_α cleavages were more prominent than cleavage of the low-energy C–N bonds, which are the favored cleavage points in CID, post-source decay and IRMPD. The residual charge had a slightly higher preference for the C-terminus product ions for the $1+$ precursor ion, but was evenly distributed between the N- and C-terminus product ions for the $2+$ charge state precursor ion. Neutral losses of OH or NH_3,

CH_4N_2, CH_5N_3 and $C_4H_{10}N_3$ (indicated with a red asterisk in Fig. 2) were observed for both the singly and doubly charged precursor ions. The latter three neutral losses are known to be indicative of side chain losses from arginine.[52,53] Singly and doubly charged precursor ions of bradykinin also revealed the side losses of serine, indicated by the cleavage of a hydroxyl radical group[54] and the loss of 17 m/z from the a_6 product ion resulting in the d_6 ion (indicated with a circle). A variety of hydrogen gains in the form of $a+1$, $x+1$ and $z+1$ ions were observed for both charge states, which was similarly observed in the latest metastable atom dissociation research of Berkout and Doroshenko in the case of $a+1$ ions.[48] In one case, a hydrogen loss resulting in an $x-1$ ion was observed for the $1+$ charge state of bradykinin. Hydrogen rearrangement is commonly observed and well characterized in ECD and can contribute to the generation of an aminoketyl radical that can then propagate along the peptide backbone.[21,55] N–C_α or C_α–C bond cleavage on the N-terminal side of the aminoketyl radical can then lead to the predominantly observed $x+1$ and $z+1$ even-electron species.

It is important to note the presence of the $2+$ product ions on exposure of the $1+$ precursor ions to metastable atoms states of helium or argon. The doubly charged product ions support the proposed mechanism of activation of singly charged peptide ions via Penning ionization.[47,50] Two fragmentations at the first proline (y_8 and x_8 ions), two fragments at the second proline (y_7 and b_2 ions) and seven fragments at the third proline (x_3, y_3, w_3, z_3-2H, z_3-CH, a_6 and b_6 ions) were observed for the singly and doubly charged precursor ions. One $a+1$ ion and one $b+1$ ion were observed for the $1+$ charge state and one $z+1$ ion in the $2+$ charge state of bradykinin.

Activation of bradykinin using the argon metastable atom beam provided at least one type of fragment ion at every amino acid for both the 1+ and 2+ precursor charge states of bradykinin. The fragmentation spectra for the two charge states were similar to the fragmentation achieved with helium in that all ion type fragments resulted. However, approximately 35% fewer fragments were observed when using argon metastable atoms. The fragment ion c_3 is the only new fragment observed in the 2+ charge state using argon metastable atoms. When fragmented with argon metastable atoms, the charge on the product ion had a slightly higher tendency to be retained on the N-terminal side of the peptide. For the doubly charged precursor ion, the charge-reduced species $[M+2H]^{+\bullet}$ was produced with a higher abundance when using argon metastable atoms as opposed to helium. Similar side chain neutral losses were observed for argon metastable activation as for helium. The loss of the serine side chain, 17 m/z, was also observed using argon metastable atoms but at a much lower intensity.

Substance P: 1+ and 2+ charge states

Figure S1 in supporting information shows fragmentation spectra of substance P collected in four different modes. The 2+ charge state, whether dissociated with helium or argon metastable atoms achieved 100% sequence coverage, yet the cleavage between the glycine and leucine was elusive when fragmenting the singly charged precursor ion using helium metastable atoms. Only five fragment ions were observed for the singly charged precursor ion on exposure to argon metastable atoms, indicating that Penning ionization with this relatively low-energy metastable atom species (11.55 or 11.72 eV) does not provide as much energy as the helium metastable atoms for inducing fragmentation. MAD fragmentation efficiencies ranged from 0.7 to 3.6% for substance P, with a total of 36 combined (both charge states and metastable gases) fragments out of 58 total possible fragments (c_1, c_3, z_8 and z_{10} are not normally possible because of the proline residues).

Fragmentation of the 2+ charge state using a helium metastable atom beam resulted in a variety of ion types (a, b, c, x, y and z) and a relatively low abundance charge-reduced species $[M+H]^+$ and $[M+2H]^{+\bullet}$. These observations were similar to those observed for bradykinin. MAD of the 1+ charge state of substance P yielded a similar number of product ions in comparison to the 2+ charge state, but with slightly more a-type ions and slightly fewer c-type ions. The small insert in Fig. S1(a) (supporting information) shows the characteristic isotopic distribution of not only a singly charged b_5 ion with a 1 m/z difference but also two doubly charged ions with a 0.5 m/z difference. Due to the basicity of the arginine residue on the N-terminus of substance P, the product ions had a twofold higher preference for a-, b- and c-type ions over x-, y- and z-type ions. The neutral losses observed for substance P were not as extensive as those observed for bradykinin; only OH or NH_3 and CH_4N_2 losses were observed (indicated with a red asterisk in Fig. S1). However, the side chain loss of 58 m/z, C_2H_4NO, from the glutamine residue[54] at position 5 resulting in the d_5 ion (indicated with a circle) is apparent in Fig. S1(a). Substance P contains two proline residues, resulting in the a_3 and b_3 ions via the fragmentation of the singly and doubly charged precursor ions with helium metastable atoms. To our knowledge, such product ions for proline residues are not common in ECD or ETD. Again, a series of a + 1, x + 1 and z + 1 ions were observed for both charge states, with one y + 1 ion in the 2+ charge state and one z − 1 ion for the 1+ charge state of substance P.

MAD of substance P using argon metastable atoms results in fragmentation that is not as extensive as observed with helium metastable atoms, especially for the singly charged precursor ion. The small insert in Fig. S1(c) shows the isotopic distribution of the $[M+H]^{2+\bullet}$ ion. The doubly charged precursor ion produced a complete c-type ion series, lacking only c_1 and c_3 that are unlikely due to the proline residues at these positions. MAD using metastable argon atoms produces ions not observed in the doubly charged peptide fragmentation with helium such as z_9, and one which is not observed in either charge states for helium, y_9. For the doubly charged precursor ion, the charge is retained almost exclusively on the N-terminus side of the product ions after fragmentation.

For bradykinin and substance P, we observed that argon metastable atom exposure generates more charge-reduced species, such as $[M+2H]^{+\bullet}$ and $[M+H]^+$, than helium metastable atom exposure. This was also observed in the work of Misharin *et al.* and is thought to be related to the fact that helium metastable atom states are closer to the ionization potential and therefore result in more exothermic electron transfer reactions – which results in more fragmentation. The doubly charged ion experienced similar neutral losses as seen with bradykinin, losing OH or NH_3, CH_4N_2 and CH_5N_3 (indicated with a red asterisk in Fig. S1). Again, the latter two neutral losses indicate the presence of arginine. When argon metastable atoms were used for the dissociation of substance P, no a + 1, x + 1, etc. ions were observed, and only one y − 1 radical ion for the 2+ charge state was observed. Argon metastable atoms therefore appeared to be less capable of promoting the migration of H atoms between product ions.

Backbone cleavage of proline residues

Fragmentation resulting in a mixture of a-, b-, c-, w-, x-, y- and z-type ions from proline, as observed here with MAD, is not at all characteristic of ECD and ETD dissociation. However, the cleavage of the $N-C_\alpha$ bond of proline has once been observed in ECD and HECD experiments by Cooper *et al.*[44] A similar z ion was observed here using MAD dissociation on the seventh amino acid proline residue of bradykinin (Fig. 3(a)). This type of fragmentation occurs through the cleavage of two covalent bonds, one on the peptide backbone ($N-C_\alpha$ bond) and one within the proline side chain (Fig. 3(c)), resulting in the ions: z_3-2H, z_3-CH and w_3 (z_3-C_2H_4). Figure 3(a) shows the three ion fragments indicative of cleavage of the proline residue in the third position of bradykinin that are observed at 402, 391 and 377 m/z, respectively. The combined observations of a-, b-, w-, x-, y- and z-ions at this residue indicate that the mechanism of fragmentation is not a simple electron transfer process, like ECD or ETD, but is instead unique to metastable atom activation. These ions were observed following MAD of either precursor charge state of bradykinin when using helium metastable atoms (Fig. 2(a and b)). In addition to bradykinin, cleavage of the proline ring was again detected in both the PHPRI and PHPRL spectra resulting in the a_2, b_2, c_2, x_3, y_3, z_3-2H, z_3-CH and w_3 ions for each peptide (Fig. 4(a and b)). The three fragments indicative of the proline ring cleavage were observed at the same m/z for both the peptides, PHPRI and PHPRL: w_3 at 342.3 m/z, z_3-CH at 357.3 m/z and z_3-2H at 368.3 m/z, as seen in Fig. 4(a and b). Figure 3(b) shows the mass spectrum of PHPRL, highlighting the z_3-2H, z_3-CH and w_3 (z_3-C_2H_4) ions.
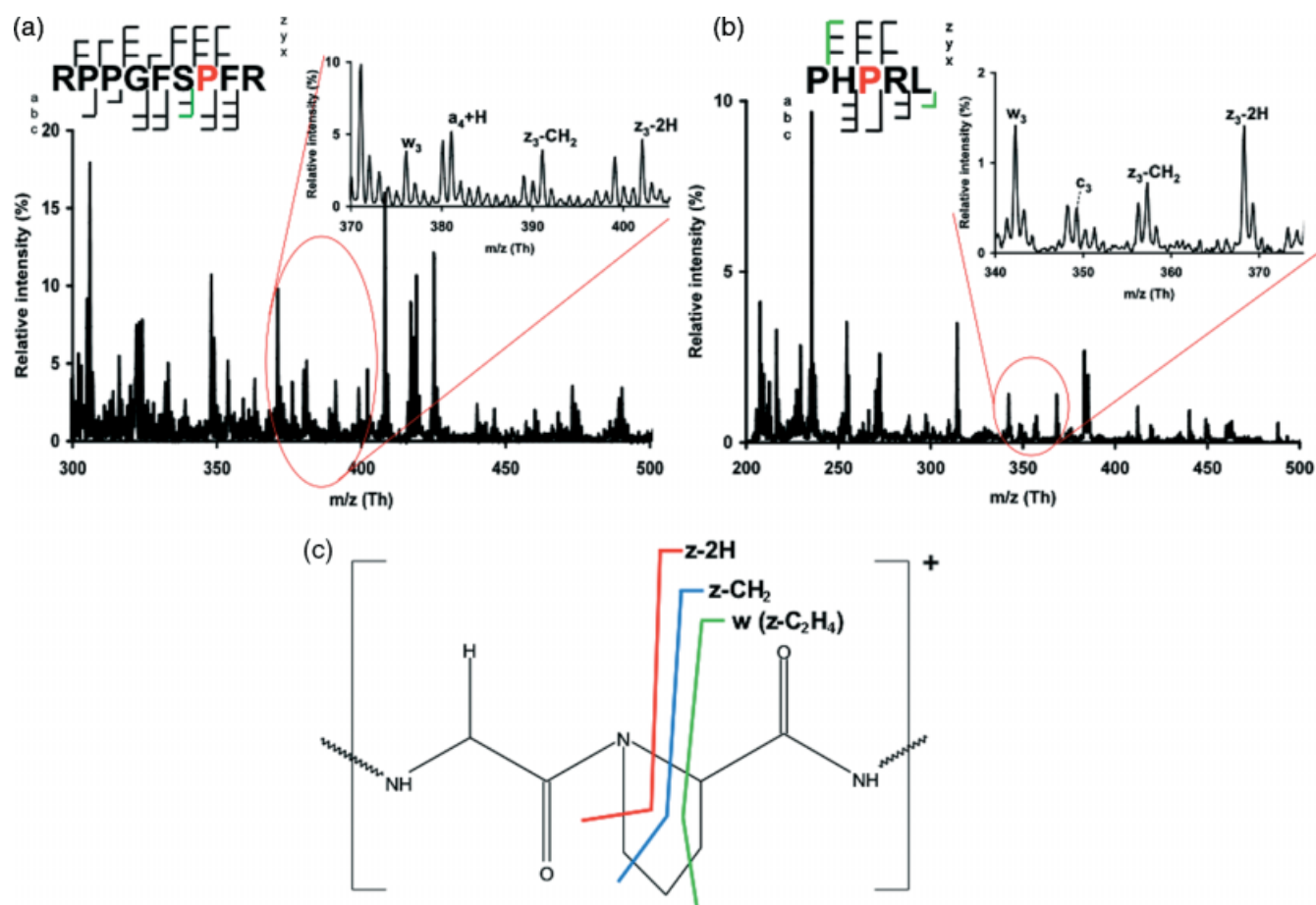
Figure 3. Metastable atom-activated dissociation spectra of (a) bradykinin and (b) the PHPRL peptide. Highlighted are the z_3-2H, z_3-CH and w_3 (z_3-C_2H_4) ions produced via the cleavage of two covalent bonds in the five-membered ring of the proline residue at position 3 in PHPRL and position 7 in bradykinin (red P indicates proline residue of interest). The two covalent bond cleavages necessary to produce the z-2H, z-CH and w (z-C_2H_4) ions are illustrated in (c).

Differentiating leucine and isoleucine

The singly charged species of peptides PHPRL and PHPRI were fragmented by helium metastable atoms, resulting in 15 different fragment ions of all ion types and a small Penning product ion, $[M+H]^{2+\bullet}$. The MAD spectrum of PHPRL shown in Fig. 4(a) has four particular peaks of interest at 229.4, 342.3, 506.3 and 463.3 m/z representing a loss of 43 m/z from the $z_2 + 1$, y_3, $x_4 + 1$ and $z_4 + 1$ ions, respectively. These ions are indicative of a neutral loss of $\bullet CH(CH_3)_2$ from the leucine side chain.[25] Fig. 4(b) is the spectrum of PHPRI that has five diagnostic peaks at 243.4, 357.4, 383.3, 520.6 and 477.4 m/z. These peaks correspond to the loss of 29 m/z from the $z_2 + 1$, $x_3 + 1$, y_3, $x_4 + 1$ and $z_4 + 1$ ions, respectively, which is indicative of the neutral loss of $\bullet CH_2CH_3$ from the isoleucine side chain.[25] Similar to ECD, MAD activation may also permit radical ion migration and fragment at more than one covalent bond. Another alternative reason for the observation of cleavage at two disparate covalent bonds is the possibility of multiple metastable atom collisions, especially at long exposure times. The d_5 ion (indicated with a circle) is present in both the PHPRL and PHPRI mass spectra that corresponds to the neutral loss of either the leucine (43 m/z) or isoleucine (29 m/z) side chains. Figure 4(c) verifies the leucine residue in the peptide by the presence of a peak at 531.4 m/z in the PHPRL spectrum, corresponding to a neutral loss of 43 m/z from the a_5 ion, which is absent in the PHPRI spectrum. Likewise, Fig. 4(d) shows a peak at

545.4 m/z in the PHPRI spectrum detecting the neutral side chain loss from isoleucine that is not present in the PHPRL spectrum. To our knowledge, this is the first report to provide evidence that MAD can distinguish between isoleucine and leucine, indicating a unique and highly beneficial capability.

Phosphorylated peptides

Angiotensin II

Phosphorylated angiotensin II has a phosphorylated tyrosine residue at position 4. The singly charged phosphopeptide ion of 1127 m/z was isolated and the fragmentation spectrum following exposure to helium metastable atoms is shown in Fig. 5. The dissociation resulted in mostly a-, b- and z-type ions. Figure 5 shows that the phosphorylation site remains mostly intact during cleavage of the amide backbone, and thereby enables phosphorylation-site determination. Tandem mass spectrometry and CID of phosphopeptides are well characterized, showing that phosphotyrosine loses HPO_3 (80 m/z) and phosphoserine loses H_3PO_4 (98 m/z).[56] Phosphotyrosine is different from phosphoserine in that cleavage tends to occur between the phosphorus and highly stable phenolic oxygen resulting in the loss of HPO_3. Our data is consistent with these reports, detecting several neutral losses of 80 m/z from the phosphotyrosine peptide fragment ions (labeled with a red asterisk), which correspond to the loss of HPO_3. However, we do detect a neutral loss of 98 m/z
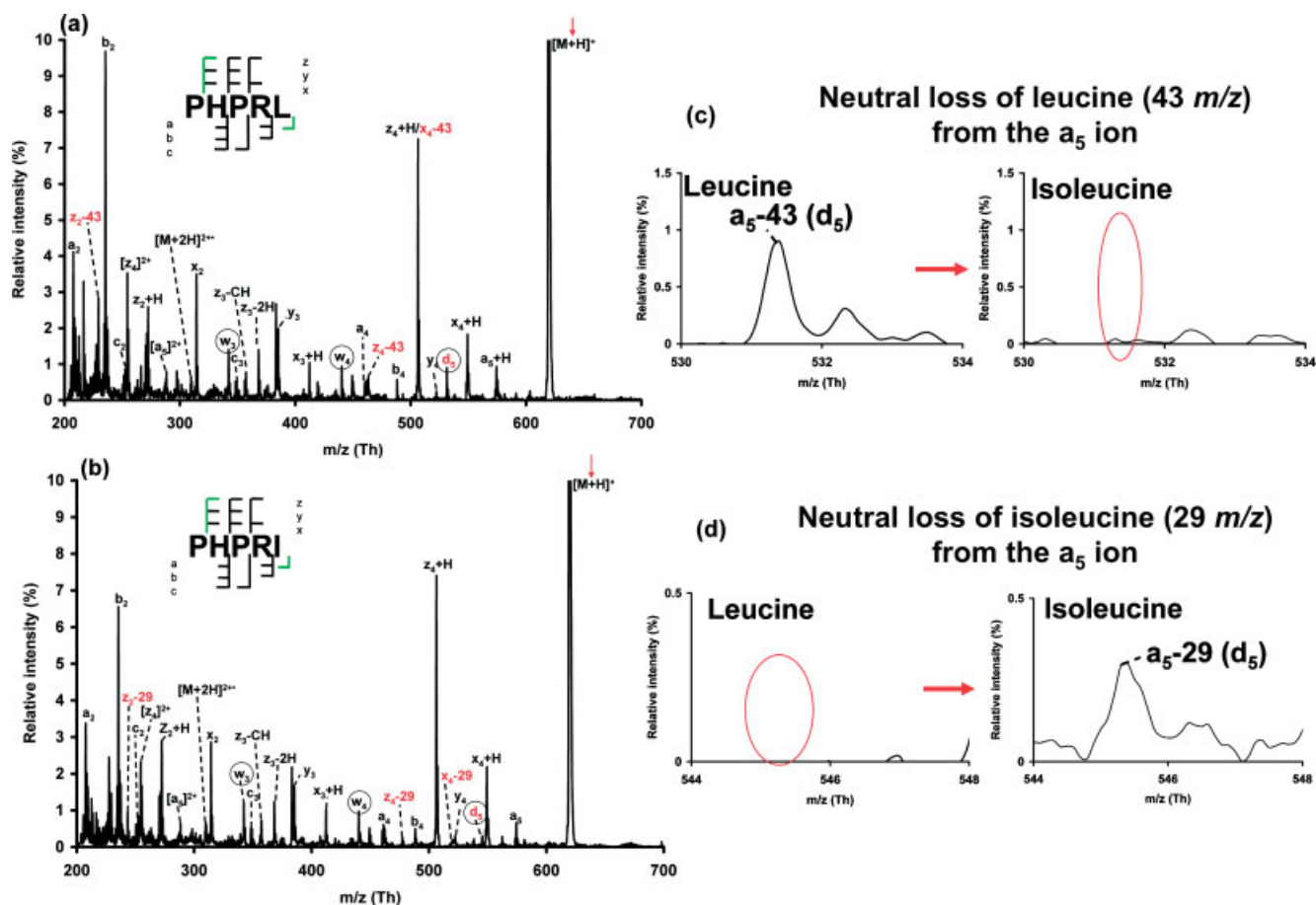
Figure 4. Metastable atom-activated dissociation spectra of the two synthetic peptides PHPRL and PHPRI: (a) $He^m + [M+H]^+$, showing several neutral losses of 49 m/z; (b) $He^m + [M+H]^+$, showing several neutral losses of 29 m/z; (c) confirming the leucine neutral loss from the z_2 and z_4 ions that are not present in the isoleucine spectrum; (d) confirming the isoleucine neutral loss from the z_2 and z_4 ions that are not present in the leucine spectrum. (Key for peptide sequencing: black line, product ions observed in 1+ charge state; green line, product ions observed in both 1+ and 2+ charge states; precursor is indicated by a red arrow; and side chain fragments are circled).
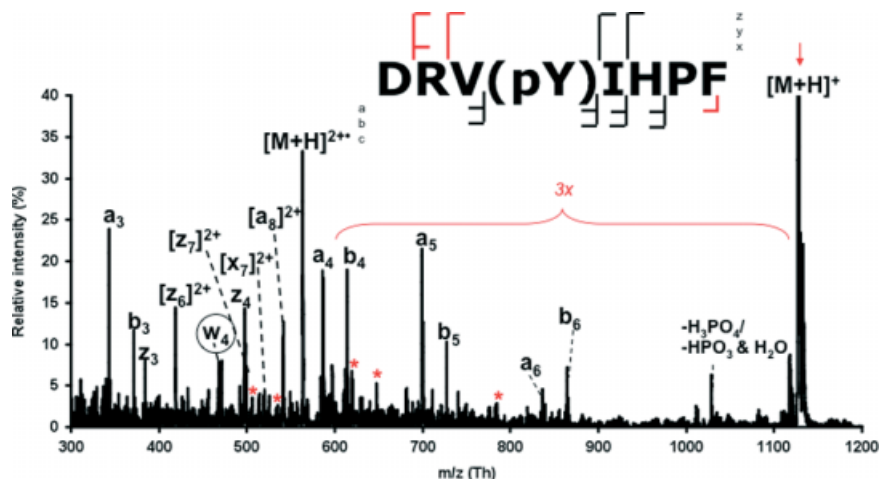
Figure 5. Metastable atom-activated dissociation spectrum of singly protonated phosphorylated angiotensin II with a helium metastable atom beam. (Key for peptide sequencing: black line, product ions observed in 1+ charge state; red line, product ions observed in 2+ charge state; red asterisk, b_6, b_5, a_5, b_4 and a_4 without the phosphate group; precursor is indicated by a red arrow; and side chain fragments are circled).

from the precursor ion, which is assigned to a sequential loss of HPO_3 and H_2O.[56] The preservation of the labile phosphate group during fragmentation is also possible with ECD and ETD, but ECD and ETD are not applicable to singly charged precursor ions, as demonstrated here for MAD activation. In addition to phosphate site determination, the isoleucine residue at position five is confirmed and differentiated from leucine by the presence of a w_4 (indicated with a circle) ion that is the result of a neutral loss of 29 m/z from the z_4 ion.

Cholecystokinin (peptide 10–20)

Phosphorylated cholecystokinin has a phosphorylated serine residue at position 6. Fragmentation of the isolated 1+ charge state (1332 m/z) by helium metastable atoms is shown in Fig. 6(a). Extensive fragmentation in the form of a-, b-, c-, x-, y- and z-type ion fragments is again observed. As with angiotensin II, the phosphate group remains mostly intact after MAD dissociation, thereby enabling phosphorylation-site determination. Again our

results are consistent with previous phosphoserine research,[56] showing several neutral losses of phosphoric acid (98 m/z) that are indicated in Fig. 6 with a red asterisk. A number of side chain cleavages were also observed, including the w_5 and d_7 ions, which confirmed the presence of the leucine residue at position 7, and the v_4 ion (indicated with a circle), which is a neutral loss of CO_2H, or 45 m/z, from aspartic acid. The spectrum shown in Fig. 6(a) is generated from an average of 50 scans, each of which is composed of 5 averaged spectra (representing 3.8 min of data acquisition). The spectrum shown in Fig. 6(b) is generated from a single scan of 5 averaged spectra, which took less than 1 s to collect. This single scan spectrum contains 54% of the identified peaks in the spectrum obtained from 50 scans, and all the information required to determine the phosphorylation site.

Peptide Anions: 2− charge state

The 2− charge state of bradykinin was exposed to a helium metastable atom beam, which resulted in 11 different ions and
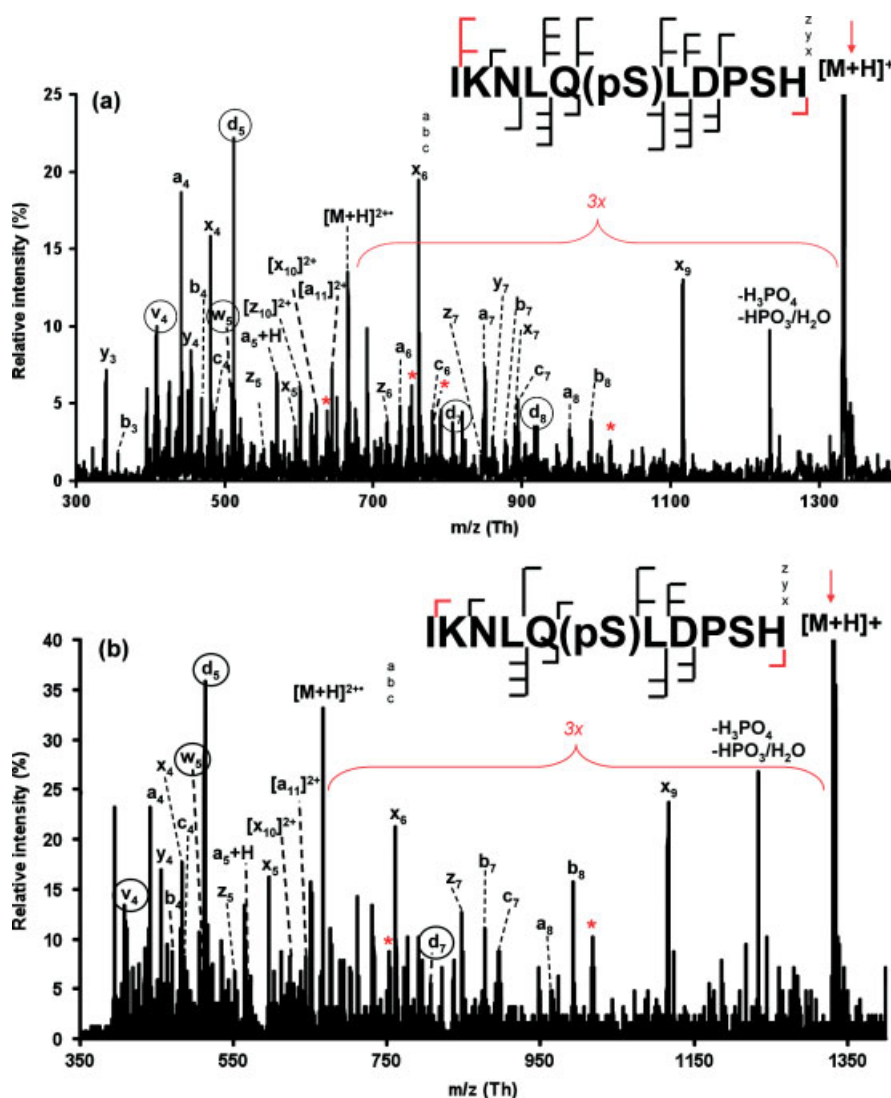

Figure 6. Metastable atom-activated dissociation spectra of singly protonated phosphorylated cholecystokinin (peptide 10–20) using a helium metastable atom beam, (a) average of 2500 spectra and (b) average of 5 spectra (a single data point), collected in ∼1 s. (Key for peptide sequencing: black line, product ions observed in 1+ charge state; red line, product ions observed in 2+ charge state; precursor is indicated by a red arrow; and side chain fragments are circled).

a large charge-reduced product ion. The most predominant ions observed in Fig. 7 were a series of x-type ions (x_4 – x_7 and x_9), which were also observed by Misharin *et al.*[49] However, we also observed two y- and two z-type ions as well as one a- and one b-type ion. The charged-reduced product ion shows a wide isotopic distribution (shown in the insert in Fig. 7) with a predominant [M−2H]$^{-\bullet}$ peak, also observed by Misharin *et al.*[49] A neutral loss of 43 *m/z* from the charged-reduced species, [M−2H]$^{-\bullet}$ and [M−3H]$^-$, is the loss of $\bullet CH(CH_3)_2$ from the leucine side chain located at position 10 (indicated with an asterisk in Fig. 7). Fragmentation efficiencies for MAD of anionic substance P exceeded 7%, almost doubling the efficiencies observed for cationic MAD. Similar results were observed for fibrinopeptide B (data not shown); a series of x-type ions (x_6 – x_9 and x_{11} – x_{13}), one a-type ion, and the charged-reduced ion were produced from the precursor ion, [M−2H]$^{2-}$.

Kinetic study of 1+ and 2+ charge states of bradykinin

Internal energy deposition during MAD was explored using both the singly and doubly charged ion states of bradykinin. Helium metastable atom pulse lengths from 50 to 250 ms generated at kinetic energies between 6 and 10 keV were used. As expected, with increasing metastable atom pulse length and increasing

kinetic energy, the precursor ion intensity of both the singly and doubly charged states decreased (data not shown), indicating that precursor ions are indeed reacted away during the experiments. Figure 8(a and b) show the effect of pulse length and kinetic energy of the metastable atom pulse on the observed intensity of the z_4+ H ion for the singly and doubly charge states, respectively. Longer pulse lengths are optimal at lower metastable atom kinetic energies producing the greatest number of fragments, whereas shorter lengths are optimal at higher kinetic energies. Regardless of pulse length, kinetic energies above 9 and below 6 keV produce spectra with low signal-to-noise ratio (data not shown), with limited detectable fragmentation. Figure 9 shows the a_3, c_5 and y_8 product ion intensities at different pulse widths at the same kinetic energy of 7 keV. The singly charge species was optimal with pulse lengths above 200 ms, yet the doubly charged species (data not shown) required a shorter pulse length (on average between 100 and 150 ms) for maximum fragmentation intensity. The intensity of the Penning product ion is highest using kinetic energies of 8 keV at pulse widths between 200 and 250 ms. The charge-reduced ion (data not shown) had the highest intensity at kinetic energies between 6 and 7 keV, which is 1 keV lower than the optimal kinetic energy of the fragment product ions generated from the singly charge state. The data generated from the a_3, b_4,
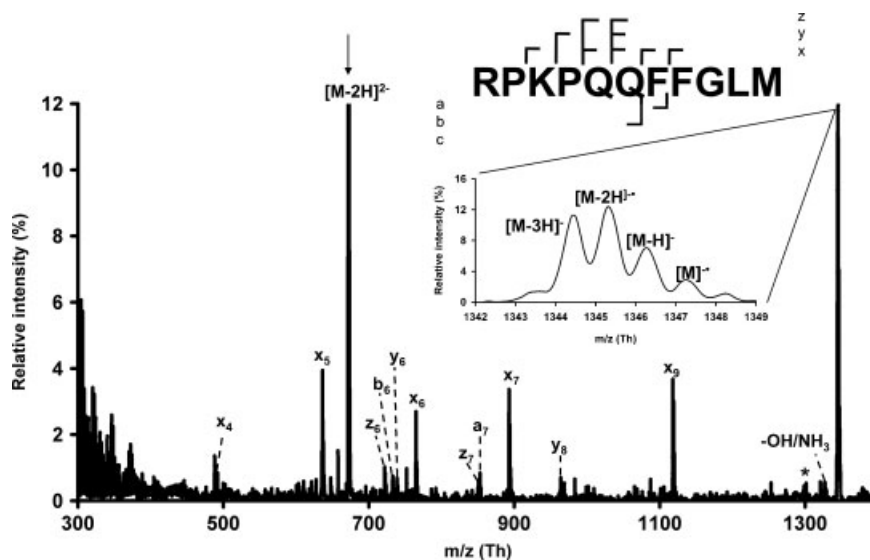

Figure 7. Metastable atom-activated dissociation spectrum of doubly deprotonated substance P using a helium metastable atom beam. The insert shows the isotopic distribution of the charged-reduced species.
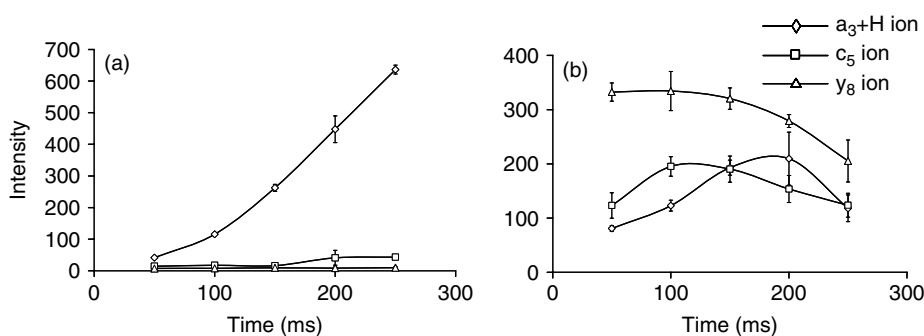

Figure 8. Relationship of how helium metastable atom pulse time and voltage applied to fast atom bombardment gun anode affects fragmentation of singly and doubly charged bradykinin: (a) fragmentation intensity of the z_4+ H ion at 50, 100, 150, 200 and 250 ms metastable atom exposure using 7, 8, 9 and 10 keV on the [M+H]$^+$ species and (b) on the [M+2H]$^{2+}$ species.
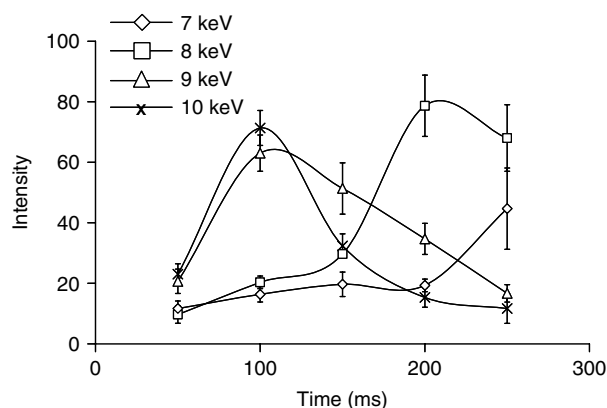
Figure 9. Fragmentation intensity of a_3+ H ion (324.3 m/z), c_5 ion (573.4 m/z) and y_8 ion (904.4 m/z) using 7 keV after 50, 100, 150, 200 and 250 ms metastable atom beam exposures on the $[M+H]^+$ species of bradykinin.

z_4, c_5, x_6 and y_8 ions (not all data shown) showed that signals for the $C_\alpha - C$, $N - C_\alpha$ and $C - N$ backbone bond cleavages are optimized at approximately the same conditions.

Proposed mechanism of metastable atom activation

Misharin *et al*. have already proposed an electron transfer reaction mechanism for charge-reduction of polyprotonated peptide cations with metastable atoms.[49] Our group[50] and Berkout and Doroshenko[48] have also proposed a mechanism for the Penning ionization of polyanionic peptide ions. Our results are consistent with these proposed mechanisms. Reactions between metastable atoms and singly protonated peptide cations, as observed here and elsewhere,[48] result in several possible outcomes, one of which is the Penning ionization[57–59] of the protonated peptide ion (P),

$$[P + nH^+]^{n+} + M^* \leftrightarrow [P + nH^+]^{(n+1)+\bullet} + M + e^- \quad (1)$$
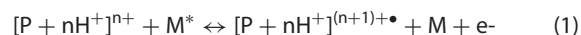
Where M is a noble gas atom. This reaction leads to the generation of a radical cation, which is known to be more reactive than even-electron cations. This type of process has been shown to be accompanied by electronic excitation, rearrangement and subsequent fragmentation when neutrals are used as the precursors.[48,50] Ohno *et al*.[60] have also shown that neutral targets of Penning ionization are preferentially ionized at surface-exposed regions of high electron density, such as the lone pairs of electrons on carbonyl oxygen atoms.

Scheme 1, shows a McLafferty rearrangement[61] for protonated dialanine as an example of the type of fragmentation that can follow Penning ionization of singly charged peptide cations. This reaction occurs via hydrogen transfer from the γ-position followed by bond cleavage of the β-bond, thus creating c- or z-type ions. The reaction is simplified as a concerted mechanism in the scheme. Scheme 2 shows another potential pathway for the rearrangement/fragmentation of radical cations. This fragmentation occurs via α-cleavage. These schemes show that several different possible rearrangement/fragmentation pathways following metastable activation result in cleavage of the amide backbone, with the possible generation of a-/x- and c-/z-type ions, in addition to the commonly observed rearrangement b-/y-type products observed through collisional activation. Another occurrence is the charge-reduction of doubly protonated peptide cations from an electron transfer through ion-metastable atom collisions resulting in $[M+2H]^{+\bullet}$. Subsequently, the ejection of a radical hydrogen atom forms the $[M+H]^+$ charge-reduced product ion, as seen with substance P. Our product ion spectra show all types of product ions (a-, b-, c-, d-, x-, y-, z-, w- and v-) indicating that an extensive variety of competing mechanisms are also observable.

Conclusion

MAD of bradykinin and substance P resulted in abundant levels of a-, b-, c-, x-, y- and z-type ions for both precursor charge states regardless of the type (argon or helium) of metastable atoms used. Substance P contains two basic residues close to the N-terminus, which favors the production of a-, b- and c-type ions over C-terminal ions. Bradykinin showed no specific preference for C-terminal and N-terminal product ions. A series of x-type ions were produced for both anionic substance P and fibrinopeptide B. MAD of the two phosphopeptide cations, angiotensin II and cholecystokinin, produced an extensive amount of ions while leaving the labile phosphate group mostly intact after dissociation that readily enabled phosphorylation-site determination. Leucine and isoleucine were successfully differentiated in several peptides through the neutral loss of their side chain, resulting in several different distinct fragment ions for either leucine or isoleucine. We have successfully shown that MAD-MS can result in more than 100% sequence coverage with MAD fragmentation efficiencies approaching 4% for cationic peptides and 7% for anionic peptides and provide a variety of a-, b-, c-, x-, y- and z-type ions with frequent side chain fragmentation. This novel dissociation method therefore appears to be an interesting and complementary alternative to ECD, ETD and CID, especially for singly charged precursor
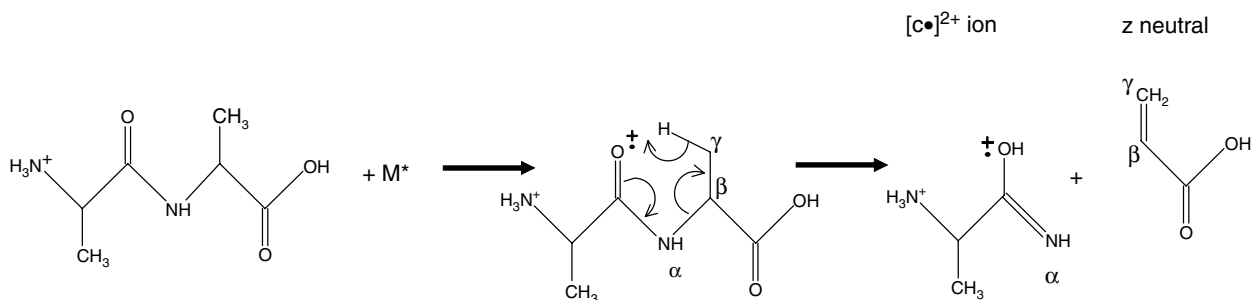
Scheme 1. Possible outcome from Penning ionization (PI) of dialanine $[AA+H]^{1+}$. PI leads to a radical cation on the carbonyl oxygen atom that follows a McLafferty rearrangement to provide β-cleavage of the amide backbone to create c-/z-type fragments. Only one outcome is shown, but the original charging proton is independent of the reaction chemistry and may reside on either of the product ions.

www.interscience.wiley.com/journal/jms
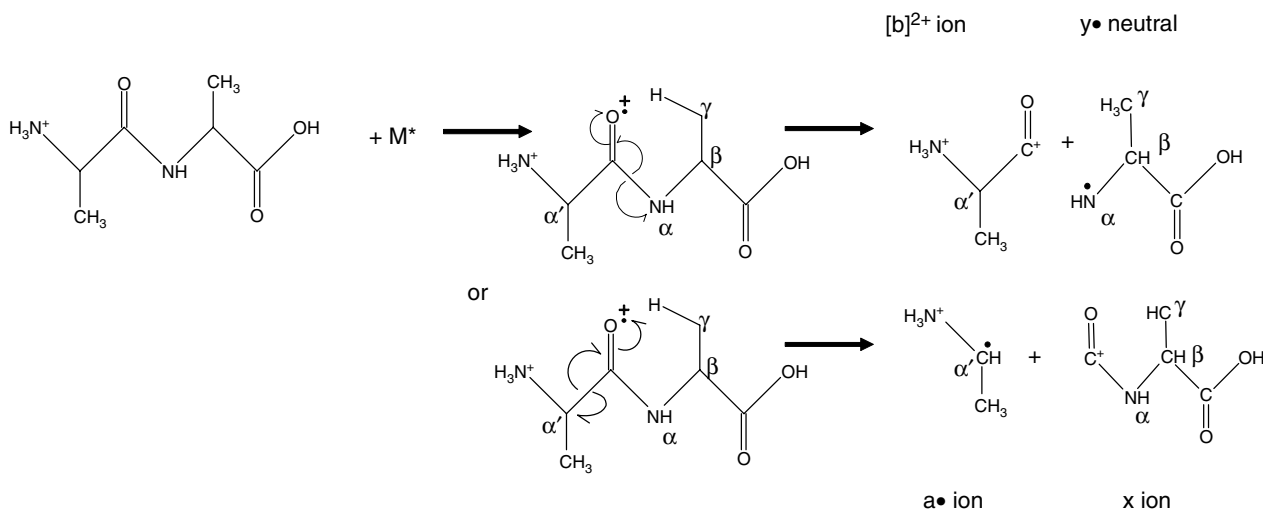
Scheme 2. Alternative outcome from Penning ionization (PI) of dialanine $[AA+H]^{1+}$. PI leads to a radical cation on the carbonyl oxygen atom that fragments through α-cleavage of the amide backbone to create a-/x- or b-/y-type fragments. b-/y-type ions can also form through the more-common cyclization mechanism (not shown).[62] The original charging proton is independent of the reaction chemistry and may reside on either of the product ions, thereby affecting the observed product ions.

ions. Another distinct advantage is the ability to utilize relatively low-cost ion trap instrumentation to perform these extensive fragmentations, as opposed to expensive FT-ICR instruments that are commonly employed for ECD fragmentation.

Supporting information

Supporting information may be found in the online version of this article.

References

[1] K. L. Busch, G. L. Glish, S. A. McLuckey. *Mass Spectrometry/Mass Spectrometry: Techniques and Applications of Tandem Mass Spectrometry*, VCH Publishers: New York, **1988**.

[2] J. Laskin, J. H. Futrell. Collisional activation of peptide ions in FT-ICR mass spectrometry. *Rapid Communications in Mass Spectrometry* **2003**, *17*, 2694.

[3] R. C. Dunbar, T. B. McMahon. Activation of unimolecular reactions by ambient blackbody radiation. *Science* **1998**, *279*, 194.

[4] J. L. Stephenson Jr, R. A. Yost. Photodissociation in the ion trap. In *Practical Aspects of Ion Trap Mass Spectrometry*, vol. 2, Chapter 5, R. E. March, J. F. J. Todd (eds). CRC Press: New York, **1995**.

[5] Z. Q. Guan, N. L. Kelleher, P. B. O'Connor, D. J. Aaserud, D. P. Little, F. W. McLafferty. 193 nm photodissociation of larger multiply-charged biomolecules. *International Journal of Mass Spectrometry* **1996**, *158*, 357.

[6] D. P. Little, J. P. Speir, M. W. Senko, P. B. O'Connor, F. W. McLafferty. Infrared multiphoton dissociation of large multiply-charged ions for biomolecule sequencing. *Analytical Chemistry* **1994**, *66*, 2809.

[7] W. J. Herron, D. E. Goeringer, S. A. McLuckey. Gas-phase electron-transfer reactions from multiply-charged anions to rare-gas cations. *Journal of the American Chemical Society* **1995**, *117*, 11555.

[8] R. A. Zubarev, N. L. Kelleher, F. W. McLafferty. Electron capture dissociation of multiply charged protein cations. A nonergodic process. *Journal of the American Chemical Society* **1998**, *120*, 3265.

[9] L. Sleno, D. A. Volmer. Ion activation methods for tandem mass spectrometry. *Journal of Mass Spectrometry* **2004**, *39*, 1091.

[10] E. A. Kapp, F. Schutz, G. E. Reid, J. S. Eddes, R. L. Moritz, R. A. J. O'Hair, T. P. Speed, R. J. Simpson. Mining a tandem mass spectrometry database to determine the trends and global factors influencing peptide fragmentation. *Analytical Chemistry* **2003**, *75*, 6251.

[11] B. Paizs, S. Suhai. Towards understanding the tandem mass spectra of protonated oligopeptides. 1: mechanism of amide bond cleavage. *Journal of the American Society for Mass Spectrometry* **2004**, *15*, 103.

[12] A. Schlosser, W. D. Lehmann. Special feature: commentary – five-membered ring formation in unimolecular reactions of peptides: a key structural element controlling low-energy collision-induced dissociation of peptides. *Journal of Mass Spectrometry* **2000**, *35*, 1382.

[13] D. L. Tabb, L. L. Smith, L. A. Breci, V. H. Wysocki, D. Lin, J. R. Yates. Statistical characterization of ion trap tandem mass spectra from doubly charged tryptic peptides. *Analytical Chemistry* **2003**, *75*, 1155.

[14] S. A. McLuckey, D. E. Goeringer. Slow heating methods in tandem mass spectrometry. *Journal of Mass Spectrometry* **1997**, *32*, 461.

[15] M. He, G. E. Reid, H. Shang, G. U. Lee, S. A. McLuckey. Dissociation of multiple protein ion charge states following a single gas-phase purification and concentration procedure. *Analytical Chemistry* **2002**, *74*, 4653.

[16] J. M. Hogan, S. A. McLuckey. Charge state dependent collision-induced dissociation of native and reduced porcine elastase. *Journal of Mass Spectrometry* **2003**, *38*, 245.

[17] K. A. Newton, P. A. Chrisman, G. E. Reid, J. M. Wells, S. A. McLuckey. Gaseous apomyoblobin ion dissociation in a quadrupole ion trap: $[M+2H](2^+)$-$[M+21H](21^+)$. *International Journal of Mass Spectrometry* **2001**, *212*, 359.

[18] A. J. Creese, H. J. Cooper. Liquid chromatography electron capture dissociation tandem mass spectrometry (LC-ECD-MS/MS) *versus* liquid chromatography collision-induced dissociation tandem mass spectrometry (LC-CID-MS/MS) for the identification of proteins. *Journal of the American Society for Mass Spectrometry* **2007**, *18*, 891.

[19] D. M. Horn, Y. Ge, F. W. McLafferty. Activated ion electron capture dissociation for mass spectral sequencing of larger (42 kDa) proteins. *Analytical Chemistry* **2000**, *72*, 4778.

[20] H. Satake, H. Hasegawa, A. Hirabayashi, Y. Hashimoto, T. Baba. Fast multiple electron capture dissociation in a linear radio frequency quadrupole ion trap. *Analytical Chemistry* **2007**, *79*, 8755.

[21] N. Leymarie, C. E. Costello, P. B. O'Connor. Electron capture dissociation initiates a free radical reaction cascade. *Journal of the American Chemical Society* **2003**, *125*, 8949.

[22] N. A. Kruger, R. A. Zubarev, B. K. Carpenter, N. L. Kelleher, D. M. Horn, F. W. McLafferty. Electron capture *versus* energetic dissociation of protein ions. *International Journal of Mass Spectrometry* **1999**, *183*, 1.

[23] R. A. Zubarev, D. M. Horn, E. K. Fridriksson, N. L. Kelleher, N. A. Kruger, M. A. Lewis, B. K. Carpenter, F. W. McLafferty. Electron capture dissociation for structural characterization of multiply charged protein cations. *Analytical Chemistry* **2000**, *72*, 563.

[24] R. A. Zubarev. Reactions of polypeptide ions with electrons in the gas phase. *Mass Spectrometry Reviews* **2003**, *22*, 57.

[25] F. Kjeldsen, K. F. Haselmann, E. S. Sorensen, R. A. Zubarev. Distinguishing of Ile/Leu amino acid residues in the PP3 protein by (hot) electron capture dissociation in Fourier transform ion cyclotron resonance mass spectrometry. *Analytical Chemistry* **2003**, *75*, 1267.

[26] G. L. Glish, S. Ito, T. Baba, J. M. Bushey, N. Manri, H. Satake, T. Sakamoto, M. Watanabe, K. Yamada, K. Deguchi, H. Nakagawa. Liquid chromatography – tandem mass spectrometry using ion trap based electron capture dissociation. *56th ASMS Conference on Mass Spectrometry and Allied Topics*, Denver, CO, **2008**.

[27] T. F. Greene, J. M. Bushey, T. Baba, G. L. Glish. Electron detachment dissociation in a hybrid radio frequency linear ion trap/time of flight mass spectrometer. *56th ASMS Conference on Mass Spectrometry and Allied Topics*, Denver, CO, **2008**.

[28] J. J. Coon, J. E. P. Syka, J. C. Schwartz, J. Shabanowitz, D. F. Hunt. Anion dependence in the partitioning between proton and electron transfer in ion/ion reactions. *International Journal of Mass Spectrometry* **2004**, *236*, 33.

[29] J. E. P. Syka, J. J. Coon, M. J. Schroeder, J. Shabanowitz, D. F. Hunt. Peptide and protein sequence analysis by electron transfer dissociation mass spectrometry. *Proceedings of the National Academy of Sciences of the United States of America* **2004**, *101*, 9528.

[30] D. M. Good, M. Wirtala, G. C. McAlister, J. J. Coon. Performance characteristics of electron transfer dissociation mass spectrometry. *Molecular and Cellular Proteomics* **2007**, *6*, 1942.

[31] D. L. Swaney, G. C. McAlister, M. Wirtala, J. C. Schwartz, J. E. P. Syka, J. J. Coon. Supplemental activation method for high-efficiency electron-transfer dissociation of doubly protonated peptide precursors. *Analytical Chemistry* **2007**, *79*, 477.

[32] S. J. Pitteri, P. A. Chrisman, S. A. McLuckey. Electron-transfer ion/ion reactions of doubly protonated peptides: effect of elevated bath gas temperature. *Analytical Chemistry* **2005**, *77*, 5662.

[33] J. L. Stephenson Jr, S. A. McLuckey. Charge reduction of oligo-nucleotide anions via gas-phase electron transfer to xenon cations. *Rapid Communications in Mass Spectrometry* **1997**, *11*, 875.

[34] M. Scigelova, A. Makarov. Orbitrap mass analyzer – overview and applications in proteomics. *Proteomics* **2006**, *6*, 16.

[35] G. C. McAlister, D. Phanstiel, D. M. Good, W. T. Berggren, J. J. Coon. Implementation of electron-transfer dissociation on a hybrid linear ion trap-orbitrap mass spectrometer. *Analytical Chemistry* **2007**, *79*, 3525.

[36] F. Kjeldsen, O. A. Silivra, I. A. Ivonin, K. F. Haselmann, M. Gorshkov, R. A. Zubarev. C-alpha-C backbone fragmentation dominates in electron detachment dissociation of gas-phase polypeptide polyanions. *Chemistry-A European Journal* **2005**, *11*, 1803.

[37] B. A. Budnik, K. F. Haselmann, R. A. Zubarev. Electron detachment dissociation of peptide di-anions: an electron-hole recombination phenomenon. *Chemical Physics Letters* **2001**, *342*, 299.

[38] R. A. Zubarev, M. M. Savitski, E. M. Fung. New trends in ECD/ETD applications. *56th ASMS Conference on Mass Spectrometry and Allied Topics*, Denvor, CO, **2008**.

[39] A. Armirotti, E. Millo, G. Damonte. How to discriminate between leucine and isoleucine by low energy ESI-TRAP MSn. *Journal of the American Society for Mass Spectrometry* **2007**, *18*, 57.

[40] R. S. Johnson, S. A. Martin, K. Biemann, J. T. Stults, J. T. Watson. Novel fragmentation process of peptides by collision-induced decomposition in a tandem mass-spectrometer – differentiation of leucine and isoleucine. *Analytical Chemistry* **1987**, *59*, 2621.

[41] T. Nakamura, H. Nagaki, Y. Ohki, T. Kinoshita. Differentiation of leucine and isoleucine residues in peptides by consecutive reaction mass-spectrometry. *Analytical Chemistry* **1990**, *62*, 311.

[42] W. A. Tao, L. M. Wu, R. G. Cooks. Differentiation and quantitation of isomeric dipeptides by low-energy dissociation of copper(II)-bound complexes. *Journal of the American Society for Mass Spectrometry* **2001**, *12*, 490.

[43] J. L. Seymour, F. Turecek. Distinction and quantitation of leucine-isoleucine isomers and lysine-glutamine isobars by electrospray ionization tandem mass spectrometry (MSn, n = 2, 3) of copper(II)-diimine complexes. *Journal of Mass Spectrometry* **2000**, *35*, 566.

[44] H. J. Cooper, R. R. Hudgins, K. Hakansson, A. G. Marshall. Secondary fragmentation of linear peptides in electron capture dissociation. *International Journal of Mass Spectrometry* **2003**, *228*, 723.

[45] K. M. Choi, S. H. Yoon, M. L. Sun, J. Y. Oh, J. H. Moon, M. S. Kim. Characteristics of photodissociation at 193 nm of singly protonated peptides generated by matrix-assisted laser desorption ionization (MALDI). *Journal of the American Society for Mass Spectrometry* **2006**, *17*, 1643.

[46] L. A. Breci, D. L. Tabb, J. R. Yates, V. H. Wysocki. Cleavage N-terminal to proline: analysis of a database of peptide tandem mass spectra. *Analytical Chemistry* **2003**, *75*, 1963.

[47] V. D. Berkout. Fragmentation of protonated peptide ions via interaction with metastable atoms. *Analytical Chemistry* **2006**, *78*, 3055.

[48] V. D. Berkout, V. M. Doroshenko. Fragmentation of phosphorylated and singly charged peptide ions via interaction with metastable ions. *International Journal of Mass Spectrometry* **2008**, *278*, 150.

[49] A. S. Misharin, O. A. Silivra, F. Kjeldsen, R. A. Zubarev. Dissociation of peptide ions by fast atom bombardment in a quadrupole ion trap. *Rapid Communications in Mass Spectrometry* **2005**, *19*, 2163.

[50] O. Collin, G. P. Jackson. Metastable-activated dissociation mass spectrometry (MAD-MS): a new paradigm for tandem mass spectrometry. *53rd ASMS Conference on Mass Spectrometry and Allied Topics*, San Antonio, TX, **2005**.

[51] R. A. Yost, D. D. Fetterolf. Tandem mass-spectrometry (MS/MS) instrumentation. *Mass Spectrometry Reviews* **1983**, *2*, 1.

[52] H. J. Cooper, R. R. Hudgins, K. Hakansson, A. G. Marshall. Characterization of amino acid side chain losses in electron capture dissociation. *Journal of the American Society for Mass Spectrometry* **2002**, *13*, 241.

[53] H. J. Cooper, K. Hakansson, A. G. Marshall. The role of electron capture dissociation in biomolecular analysis. *Mass Spectrometry Reviews* **2005**, *24*, 201.

[54] M. M. Savitski, M. L. Nielsen, R. A. Zubarev. Side-chain losses in electron capture dissociation to improve peptide identification. *Analytical Chemistry* **2007**, *79*, 2296.

[55] M. M. Savitski, F. Kjeldsen, M. L. Nielsen, R. A. Zubarev. Hydrogen rearrangement to and from radical z fragments in electron capture dissociation of peptides. *Journal of the American Society for Mass Spectrometry* **2007**, *18*, 113.

[56] S. C. Moyer, R. J. Cotter, A. S. Woods. Fragmentation of phospho-peptides by atmospheric pressure MALDI and ESI/ion trap mass spectrometry. *Journal of the American Society for Mass Spectrometry* **2002**, *13*, 274.

[57] H. Morgner. Photo- and Penning ionization of molecules in the gas phase and in the liquid phase. In *Linking the Gaseous and Condensed Phases of Matter*, L. G. Christophorouetal (ed). Plenum Press: New York, **1994**.

[58] F. M. Penning. Ionization by metastable atoms. *Naturwissenschaften* **1927**, *15*, 818.

[59] P. E. Siska. Molecular-beam studies of Penning ionization. *Reviews of Modern Physics* **1993**, *65*, 337.

[60] K. Ohno, S. Takano, K. Mase. Penning ionization electron spectroscopy of molecules containing the C=O group: aldehydes and carboxylic acids. *Journal of Physical Chemistry* **1986**, *90*, 2015.

[61] F. W. McLafferty. *Interpretation of Mass Spectra: An Introduction*. Benjamin: New York, **1967**.

[62] R. S. Johnson, S. A. Martin, K. Biemann. Collision-induced fragmentation of $(M+H)^+$ ions of peptides – side-chain specific sequence ions. *International Journal of Mass Spectrometry and Ion Processes* **1988**, *86*, 137.

1223